Study of phase behavior of epoxy asphalt binders using differential scanning calorimetry

Apostolidis, Panos; Elwardany, Michael; Andriescu, Adrian; Mensching, David J.; Youtcheff, Jack

DOI
10.1016/j.conbuildmat.2023.130566

Publication date
2023

Document Version
Final published version

Published in
Construction and Building Materials

Construction and Building Materials 369 (2023) 130566

Contents lists available at ScienceDirect

Construction and Building Materials

journal homepage: www.elsevier.com/locate/conbuildmat

Study of phase behavior of epoxy asphalt binders using differential scanning calorimetry

Panos Apostolidis [a,*], Michael Elwardany [b], Adrian Andriescu [c], David J. Mensching [d], Jack Youtcheff [d]

[a] Delft University of Technology, Faculty of Civil Engineering and Geosciences, Delft, Netherlands
[b] Florida A&M University – Florida State University, College of Engineering, Tallahassee, FL, USA
[c] SES Group & Associates, LLC at Federal Highway Administration, Turner-Fairbank Highway Research Center, McLean, VA, USA
[d] Federal Highway Administration, Turner-Fairbank Highway Research Center, McLean, VA, USA

ARTICLE INFO

Keywords:
Glass transition
Phase behavior
Miscibility
Differential scanning calorimetry

ABSTRACT

Glass transition parameters can be used to study the miscibility, or lack of it, in polymer-modified asphalt binders. In this study, the contribution of thermodynamics of mixing to glass transition was quantitatively assessed in a differential scanning calorimeter for four asphalt binders partially and fully replaced by an epoxy system. The values of heat capacity (C_p) and, subsequently the glass transition temperature (T_g) of all binders were determined to quantify the miscibility based on the entropic changes. Emphasis was also given to examining the enthalpy of mixing as a function of epoxy system composition during curing to ensure that these binders were completely crosslinked for further analyses. In all cases, the positive deviations of the measured T_g of epoxy-modified asphalt binders ($T_{g,mix}$) obtained from the ideal mixing rule led to negative values of the entropy of mixing (ΔS^c_{mix}), dictating the presence of internal repulsive forces between the asphalt and epoxy components. Softer binders were associated with binders of low deviations of $T_{g,mix}$ values from the ideal mixing rule. Lastly, the partial replacement of asphalt binders by the epoxy system increased the T_g and decreased the amount of ΔS^c_{mix}, and such performance imposes the formation of immiscible products.

1. Introduction

Asphalt binder is the most common binding material for the construction of pavements holding together>90 % of the paved highway surfaces globally. To fulfil performance requirements and agencies' demands for enhanced durability under adverse environmental conditions and high traffic volume, polymer-modified asphalt (PMA) binders have been widely adopted. This modification can be achieved by incorporating a polymer into an asphalt binder by mechanical stirring and/or chemical reaction to achieve the desired properties.

As polymer blends and dilutant systems have been of great interest recently, the thermodynamics determining the phase behavior of such systems are well established [1,2]. Previous studies also tried to transfer this knowledge to PMA binders to provide a physical explanation of some phenomena, such as the phase separation in asphalt binders [3–5]. A limited number of studies have focused on providing quantitative information on the effect of a polymer in asphalt or of the replacement effect of an asphalt binder by other binding products to develop flexible pavement materials of enhanced properties. One example is the epoxy system employed in this research, and details of it are discussed in a later section.

Glass transition can be used to evaluate the miscibility of asphalt binders and the compatibility of individual components [6–8]. The glass transition is a non-equilibrium phenomenon from an amorphous (e.g., liquid or rubbery state) into a glassy state occurring in asphalt (and other materials). This transition gradually spans over a wide temperature window, and one unique value of the glass transition temperature (T_g) is usually reported. Thus, this change is represented by a single number representing the central tendency or the average value of the glass transition range.

Different experimental techniques provide different T_g values, including differential scanning calorimetry (DSC), dilatometry, and dielectric and rheological analyses [9–12]. In this research, experiments were conducted through DSC to determine the heat capacity (C_p) and T_g values of four petroleum-based asphalt binders partially or fully replaced by an epoxy system curing by oleochemical sourced

* Corresponding author.
E-mail address: p.apostolidis@tudelft.nl (P. Apostolidis).

https://doi.org/10.1016/j.conbuildmat.2023.130566
Received 14 November 2022; Received in revised form 14 January 2023; Accepted 27 January 2023
Available online 6 February 2023

crosslinkers to quantify miscibility via the entropic changes during glass transition. Emphasis was also given to examining the enthalpy of mixing as a function of the composition of epoxy-modified asphalt (EMA) binders with curing in DSC to ensure that the studied materials were completely crosslinked without the contribution of oxygen. The theoretical background of the phase behavior of binders for flexible pavements is discussed in the following section.

2. Theoretical background

The miscibility of polymer blends is driven by the specific intermolecular interactions of individual components, such as hydrogen bond formation and π-π complex formation. A fundamental requirement for miscibility of polymer blends is that the free energy of mixing (ΔG_{mix}), which is defined by the expression in **Equation (1)**, is negative.

$$\Delta G_{mix} = \Delta H_{mix} - T\Delta S_{mix} \quad (1)$$

where T is the absolute temperature [K], ΔS_{mix} is the change in entropy of mixing [J mol^{-1} ^{o}C^{-1}], and ΔH_{mix} is the change in enthalpy of mixing [J mol^{-1}], which is the heat consumed ($\Delta H_{mix} > 0$) or released ($\Delta H_{mix} < 0$) during the mixing.

The T_g values exist as a function of the concentration of blend components (φ), providing information on whether the blends are miscible or not. Full miscibility is illustrated by detecting a single glass transition region, which indicates a blend-average, single T_g. The T_g of a miscible blend might be the mean value of the T_g of individual components of blends related to the blend composition and the ideal mixing rule. Two T_g values, independent of composition, are shown distinctly in immiscible systems.

Several approaches have been proposed using the kinetics and thermodynamics features of glass transition phenomena to predict the compositional dependence of polymer blend T_g and provide explanations for the deviations from the ideal mixing rule [13–29]. Such relationships to predict T_g compositional dependence in amorphous blends are based on the additivity for the respective properties of individual components, such as the specific volumes [13] or flexible bonds contributing to conformational changes [23]. All these equations are minor variations of the same mathematical expression, shown in Equation (2) [13]:

$$T^{eq}_{g,mix} = \frac{\varphi_A T_{g,A} + k\varphi_B T_{g,B}}{\varphi_A + k\varphi_B} \quad (2)$$

where $T^{eq}_{g,mix}$ is the $T_{g,I}$ of a binary mix predicted by the equation of interest, ϕ_I represents the concentration, expressed as either mole or weight fraction, and k is a parameter whose physical interpretation depends on the underlying predictive relationship utilized. The subscript I denotes blend components (i.e, $I = A$ for component A and $I = B$ for component B).

The determination of the compositional relationship with the T_g and its deviation can be used as indicators for the thermodynamics of mixing in amorphous systems [24]. The negative T_g deviations correspond to positive enthalpy of mixing (ΔH_{mix}), which is a measure of the energy change due to interaction. On the one hand, the T_g deviation is zero for ideal blends indicating that their constituents are compatible in all proportions (Fig. 1). The intermolecular forces are the same between the pairs of constitutive molecules; thus, there is no transfer of work or heat to or from the surroundings. On the contrary, non-ideal blends show a significant and negative ΔH_{mix} and a deviation of the ΔS_{mix}, and together with a positive T_g deviations from the corresponding ideal case, specifying materials of enhanced glass formation tendencies [13,26,30]. There may be strong differences in intermolecular forces between the constitutive molecules in such materials, even though they are not chemically reacting. Note that it was assumed no chemical reactions between the components being mixed.

The ΔS_{mix} could provide valuable information about the magnitude of intermolecular forces, mainly repulsive, in the non-ideal blends. Nevertheless, the predictive equations do not incorporate the entropy of mixing (ΔS_{mix}) even though it plays a crucial role in the glass formation of amorphous mixtures [31]. The glass transition is a phenomenon that occurs by decreasing S^c. Considering the kinetic nature of the material, the configuration of glass remains stable over infinitely long time periods at low temperatures. The glassy state configuration changes as the transition proceeds with a minimal rate toward reaching equilibrium. In a thermodynamic equilibrium state, the properties of a multi-phasic material do not change with time and do not show a tendency for spontaneous change.

The heat capacity of a binary mixture of component A and B ($T_{g,B} > T_{g,A}$) ($C_{p,mix}$) at amorphous (a) and glass (g) state is expressed in Equations **(3a) and (3b)**.

$$C^a_{p,mix} = \varphi_A C^a_{p,A} + \varphi_B C^a_{p,B} \quad (3a)$$

$$C^g_{p,mix} = \varphi_A C^g_{p,A} + \varphi_B C^g_{p,B} \quad (3b)$$

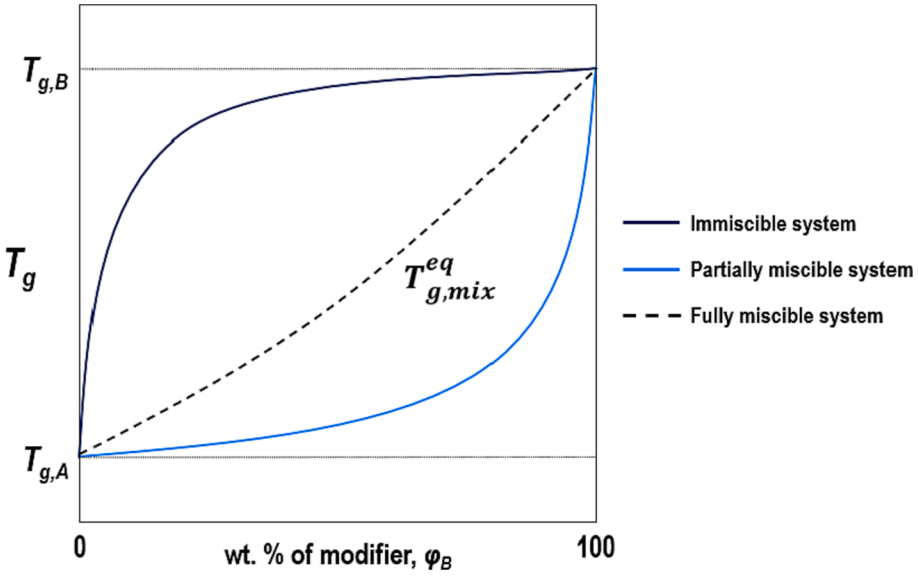

Fig. 1. Schematic representation of the composition dependence of glass transition temperature in binary systems.

The formation process of a mixture of two components, *A* and *B*, is illustrated by a cycle, as shown in Fig. 2. This cycle involves three steps in where the components are exposed to various temperatures. The initial state of the formation process is when two individual components are glassy ($T \leq T_{g,A}$), and:

- in *(i)*, the individual components are heated from temperature T to $T_{g,B}$ ($T = T_{g,B}$). During this step, the temperature passes through $T_{g,A}$ where component *A* becomes amorphous;
- in *(ii)*, the two components are mixed in the amorphous state at $T_{g,B}$; and
- in *(iii)*, the amorphous mixture is cooled down from $T_{g,B}$ to T. During this step, the mixture undergoes the glass transition at $T_{g,mix}$.

As discussed in [26], the change in entropy of each step is shown in Equations (4a), (4b), and (4c):

$$\Delta S_{(i)} = \varphi_A \int_{T}^{T_{g,A}} \frac{C^{g}_{p,A}}{T} dT + \varphi_A \int_{T_{g,A}}^{T_{g,B}} \frac{C^{a}_{p,A}}{T} dT + \varphi_B \int_{T}^{T_{g,B}} \frac{C^{a}_{p,B}}{T} dT \tag{4a}$$

$$\Delta S_{(ii)} = \Delta S_{mix} \tag{4b}$$

$$\Delta S_{(iii)} = \int_{T_{g,B}}^{T_{g,mix}} \frac{C^{a}_{p,mix}}{T} dT + \int_{T_{g,mix}}^{T} \frac{C^{g}_{p,mix}}{T} dT \tag{4c}$$

and the total change of entropy of mixing in the glassy state (ΔS^{r}_{mix}) for the whole cycle (Fig. 1) to be expressed in Equation (5) as:

$$\Delta S^{r}_{mix} = \Delta S_{(i)} + \Delta S_{(ii)} + \Delta S_{(iii)} \tag{5}$$

The ΔS_{mix} at a finite cooling rate consists of the following two parts shown in Equation (6):

$$\Delta S_{mix} = \Delta S^{c}_{mix} + \Delta S^{r}_{mix} \tag{6}$$

where ΔS^{c}_{mix} is the entropy of mixing accessible to the amorphous, or the configurational part, and ΔS^{r}_{mix} is the entropy of mixing in the vitrified mixture or the residual part. As real amorphous mixtures exhibit significant vibrational differences in relation to their glasses [32], the main characteristic of the ΔS^{r}_{mix} is inaccessible to the amorphous component when the mixture vitrifies. With the ΔS^{r}_{mix} being inaccessible to the amorphous components, the glassy state limits the possibilities of having a mixture of the same entropy equal to the summation of the entropies of individual components.

To provide an accurate link between the ΔS_{mix} of amorphous mixture and that at the glassy state, both the kinetic and thermodynamic characters of glass transition should be considered [26].

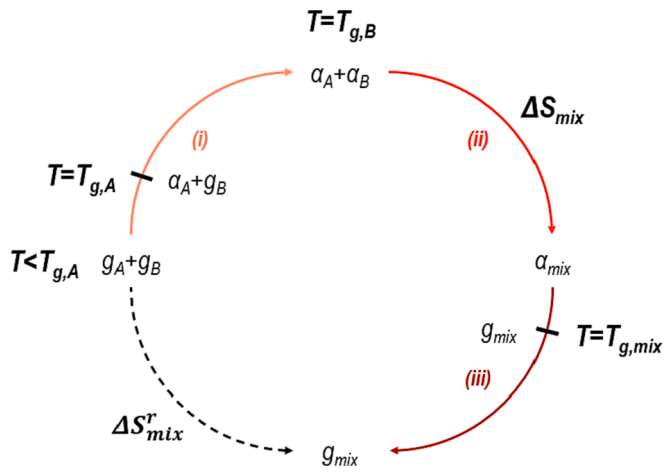

Fig. 2. Schematic representation of the thermodynamic cycle used to obtain the entropy of mixing of the glassy mixture (ΔS^{r}_{mix}).

As any thermodynamic quantity is time-independent, the changes of ΔS_{mix} at a glassy state (see Equation (5)) at an infinitely slow cooling rate is defined as shown in Equation (7):

$$\Delta S^{r}_{mix}\big|_{\infty} = \Delta S_{(i)} + \Delta S_{(ii)} + \Delta S_{(iii)} \tag{7}$$

where the superscript ∞ denotes an infinitely slow measurement.

The thermodynamic partitioning of the ΔS_{mix} is represented in Equation (8):

$$\Delta S_{mix} = \Delta S^{c}_{mix}\big|_{\infty} + \Delta S^{r}_{mix}\big|_{\infty} \tag{8}$$

The partitioning expressed by Equations (6) and (8) is visualized in Fig. 3, where the two equations are equal. Such equality frames the thermodynamic constraint of a kinetically controlled glass transition phenomenon.

Firstly, the encircled *T*-marker in Fig. 3 corresponds to the thermodynamic partitioning of the ΔS_{mix}. The dashed line denotes the $\Delta S^{c}_{mix}\big|_{\infty}$ above the zero-entropy of the mixing line, and the $T_{K,mix}$ corresponds to the point where the amount of thermally consumed entropy equals $\Delta S^{r}_{mix}\big|_{\infty}$. For a system where the separate glass components have the same entropy as the glass mixture or the differences in entropies between the amorphous- and glass-like phases become zero, the T_1 corresponds to the $T_{K,mix}$ [31]. If an amorphous component could be supercooled below its T_g, the heat capacity might be extrapolated below this temperature, and the $T_{K,mix}$ could be reached.

The encircled K-marker serves as a gauge for the decrease of ΔS_{mix} over the glass transition at finite cooling rates. The glass transition of a mixture of two components, where the ΔS_{mix} does not play any role, is denoted as $T^{eq}_{g,mix}$ in Fig. 3. Lines (Ia) and (Ib) show the case where the ΔS_{mix} does not affect the glass transition. Significantly, the ΔS_{mix} contributes to the entropy of the amorphous mixture by shifting the lines (Ia) and (Ib) upwards to (IIa) and (IIb). The $T_{g,mix}$ is where the line (IIa) changes to (IIb), and the structural equilibrium is reached. At this point, the configurational entropy cannot keep up with the pace of change in temperature at finite cooling rates, and thus glass transition occurs. The configurational entropy values of an infinitely slow test, in which the thermodynamic effects are considered, are different from those obtained at finite cooling rates (ΔS^{c}_{mix}). This behavior is also valid for the residual entropy of mixing trapped in the glass (ΔS^{r}_{mix}).

Note that the configurational entropy kinetically trapped in the glass is removed over time via structural relaxation, such as when high temperatures are applied to erase the thermal history. Considering this, the different calorimetric protocols and test timescales influence the amount of configurational entropy trapped in glasses, and subsequently, the position of the obtained glass transition shifts as such. Thus, the ΔS_{mix} contributes to the entropy for loss upon structural relaxation of the glass by an amount equal to the difference between the kinetic (ΔS^{r}_{mix}) and the thermodynamic residual entropy of mixing ($\Delta S^{r}_{mix}\big|_{\infty}$) as

$$\Delta S_{mix}\big|_{relax} = \Delta S^{r}_{mix} - \Delta S^{r}_{mix}\big|_{\infty} \tag{9}$$

By substituting Equations (4) and (6) into Equation (5), Equation (10) is yielded [26]:

$$\varphi_A \int_{T_{g,A}}^{T_{g,B}} \frac{\Delta C_{p,A}}{T} dT + \Delta S^{c}_{mix} + \int_{T_{g,B}}^{T_{g,mix}} \frac{\Delta C_{p,mix}}{T} dT = 0 \tag{10}$$

For an infinitely slow calorimetric test, the kinetic residual entropy of mixing approaches the thermodynamic residual entropy or $\Delta S^{r}_{mix} \rightarrow \Delta S^{r}_{mix}\big|_{\infty}$ and thus $T_{g,mix} \rightarrow T_{K,mix}$, and Equation (10) becomes:

$$\varphi_A \int_{T_{K,A}}^{T_{K,B}} \frac{\Delta C_{p,A}}{T} dT + \Delta S^{c}_{mix}\big|_{\infty} + \int_{T_{K,B}}^{T_{K,mix}} \frac{\Delta C_{p,mix}}{T} dT = 0 \tag{11}$$

or

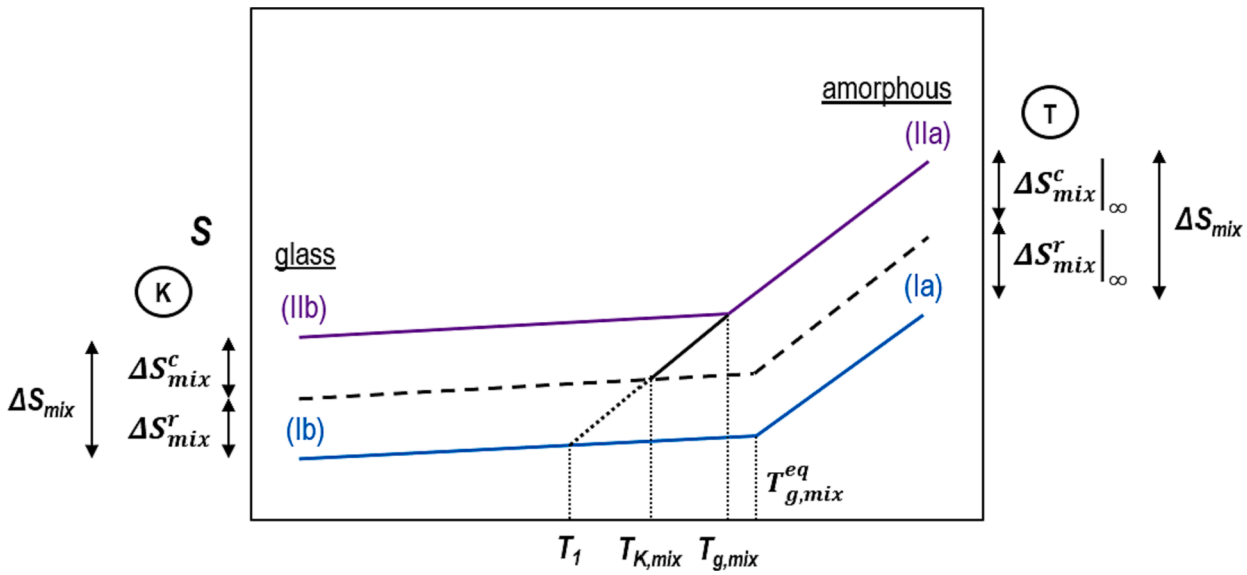

Fig. 3. Effect of the entropy of mixing on the $T_{g,mix}$ of a binary mixture.

$$\ln T_{g,mix} = \frac{\varphi_A \Delta C_{p,A} \ln T_{g,A} + \varphi_B \Delta C_{p,B} \ln T_{g,B}}{\Delta C_{p,mix}} - \frac{\Delta S^c_{mix}}{\Delta C_{p,mix}} \quad (12)$$

The first term on the right-hand side of Equation (12) corresponds to the Couchman & Karasz equation (16), which is defined as

$$\ln T^{eq}_{g,mix} = \frac{\varphi_A \Delta C_{pA} \ln T_{gA} + \varphi_B \Delta C_{pB} \ln T_{gB}}{\varphi_A \Delta C_{pA} + \varphi_B \Delta C_{pB}} \quad (13)$$

where ΔC_{pI} is the heat capacity increment of amorphous (C^a_{pI}) and glass (C^g_{pI}) of component I over the glass transition.

Hence, **Equation (12)** can be rewritten as **Equation (14)**:

$$T_{g,mix} = T^{eq}_{g,mix} \exp\left(- \frac{\Delta S^c_{mix}}{\Delta C_{p,mix}} \right) \quad (14)$$

Finally, the ΔS^c_{mix} values are obtained from the deviation from the ideal mixing rule as shown in **Equation (15)**:

$$\Delta T_{g,mix} = T^{eq}_{g,mix} \left[\exp\left(- \frac{\Delta S^c_{mix}}{\Delta C_{p,mix}} \right) - 1 \right] \quad (15)$$

The magnitude of the observed shift on T_g is kinetically controlled and is maximum for an infinitely slow calorimetric test when $\Delta S^c_{mix} \rightarrow \Delta S^c_{mix}|_\infty$.

To minimize the effect of the kinetic nature of the studied materials, a slow temperature modulated calorimetric method is implemented. The C_p and subsequently T_g values of binders will be determined based on this method, and the entropy of mixing as a function of epoxy system composition will be examined to quantify the miscibility of new binders. Further details of the temperature modulated method are provided in the next section.

3. Materials and methods

3.1. Binders

One epoxy system was employed to partially replace four petroleum-based asphalt binders: two binders from a European source (Binder 1: 70–100 pen and Binder 2: 160–220 pen), a binder from the State of Florida (Binder 3: PG 67–22) and a binder from the Commonwealth of Virginia (Binder 4: PG 64–22) (see Table 1).

The epoxy system is formulated by two liquid parts: (i) Part A, which includes epichlorohydrin-bisphenol A, and (ii) Part B, which consists of a 70 pen petroleum asphalt binder with heavy naphthenic distillates and extracts, and crosslinkers. The crosslinkers of the epoxy system are derived from oleochemical sources (e.g., animal fats, seed oils and pine trees) and are the starting materials to cure the epoxy system. The mechanical properties of the rubbery epoxy system are associated partly with the spacing of the carboxyl groups on the backbone of crosslinkers, their functionality, and their crosslink density and molecular size. Therefore, properly proportioning the crosslinkers of certain sources, functionalities, chain lengths, and molecular weights enables the formulation of the desired epoxy systems. The proportioning of the carboxyl groups' spacing on the crosslinker backbone (e.g., long and short spacing) also plays a critical role in building the target properties.

Table 1
The base asphalt binders.

Material	Binder 1	Binder 2	Binder 3	Binder 4
Grading	70–100 pen	160–220 pen	PG 67–22	PG 64–22

Here, the epoxy system samples were prepared by mixing Part A and Part B at a weight ratio of 20:80. Then, the epoxy system was added to the four asphalt binders at different weight percentages; 20 and 50 % wt of the total mass of new binder. Details of the exact preparation procedure are given in (8). Two replicates per case materials were assessed in this study.

3.2. Differential scanning calorimetry

DSC measures heat flow into and out of a material under a scanning mode of continuous temperature change. A DSC unit consists of twin calorimeters engulfed into a furnace block to minimize the heat losses and permit measurements in either temperature-linear (TL) or temperature-modulated (TM) differential scanning mode. Even when the same technique is used, different T_g values can be obtained by implementing different methods (e.g., heat flux and power compensation calorimeters) and protocols (temperature linear and modulated scanning programs) (7).

A typical calorimeter consists of a small pan of high heat conduction, usually aluminum, with a temperature sensor underneath to monitor the temperature changes. The sample calorimeter encloses the material of interest into a pan, and the reference one consists of an identical pan without any material in it, as shown in Fig. 4**a**. The methodology implemented to determine the heat capacity (C_p), the heat of mixing

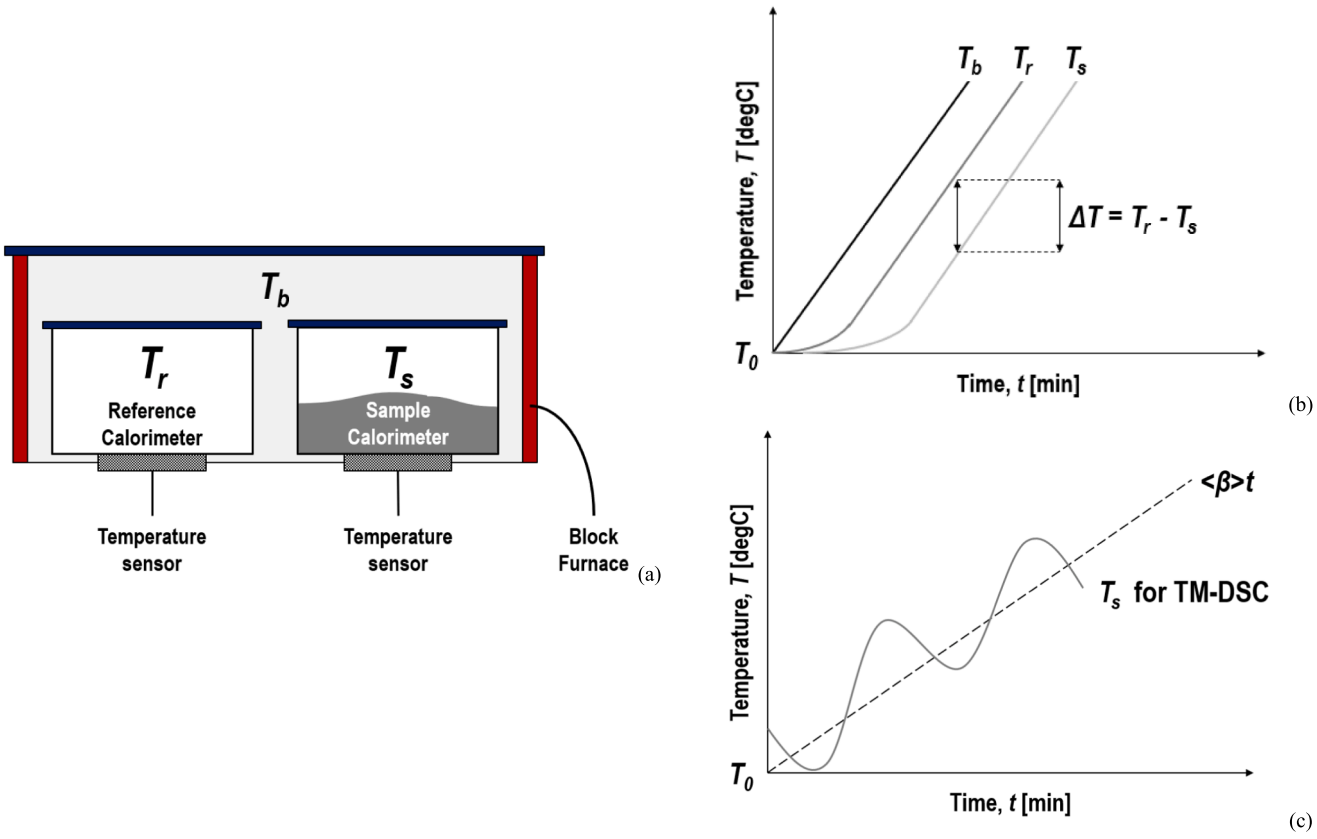

Fig. 4. Differential scanning calorimetry: (a) schematic representation, and two heating scans (b) TL-DSC and (c) TM-DSC.

(ΔH_m), and glass transition temperature (T_g) of studied binders is presented in the following sub-sections.

3.2.1. Determination of heat capacity

The amount of heat needed to change the temperature of a material by 1 °C is defined as the heat capacity. Over differential heating of twin calorimeters, the temperature of the furnace block (T_b) increases linearly, leading to an increase in temperature of reference (T_r) and sample (T_s) calorimeters, as illustrated in Fig. 4**b**. The T_b, T_r, and T_s temperatures increase with the same heating rate, lagging mainly due to pans and the heat capacity of samples. The heat capacity of the sample calorimeter (c_p) is determined as shown in **Equation (16)**:

$$c_p = K\frac{(T_r - T_s)}{\beta} = K\frac{\Delta T}{\beta} \tag{16}$$

where K is the Newton's law constant [$J{\cdot}^oC^{-1}{\cdot}min^{-1}$], which is dependent on the thermal conductance from the block furnace to the two calorimeters, and β is the heating rate [$^oC{\cdot}min^{-1}$].

It is significant to mention that heat capacity should be determined only when the steady-state is reached to minimize contribution of the scanning sample's kinetic characteristics for the reasons discussed in the **Theoretical Background** section of the manuscript. Both reference and sample calorimeters' heat flow rates are affected exclusively by the temperature change rate and heat capacities [33]. Hence, the heat capacity of a sample over a TL scan at a steady state can be expressed in **Equation (17)**:

$$mC_p = K\frac{\Delta T}{\beta} + C_s\left(\frac{d\Delta T}{dT_s}\right) \tag{17}$$

where m is the sample mass, C_p is the specific heat capacity of a sample [$J{\cdot}^oC^{-1}{\cdot}g^{-1}$], C_s is the sample's total heat capacity with the pan.

The situation differs when a periodic temperature change is superimposed on the underlying scanning rate. The addition of modulation to the temperature change could reduce heat losses, further providing higher accuracy for determining heat capacity [34]. As indicated earlier, the kinetic nature of glass transition in $T_{g,mix}$ and ΔS^c_{mix} varies with the calorimetric test timescale, but this effect is minimized with the TM scans. An example case of a small periodic component to the TL ramp $< \beta > t$ is shown in Fig. 4**c**, and the expression that describes the TM for the block furnace is defined in Equation (18):

$$T_b(t) = T_0 + \langle\beta\rangle t + A_{T_b}\sin\omega t \tag{18}$$

where T_0 is the isotherm at the beginning of the TM scan, and ω is the modulation frequency which is equal to $2\pi/p$ [rad s^{-1}], with p representing the length of one cycle [*sec*]. Similarly, T_s or T_r are expressed by **Equation (18),** with an additional phase shift added to the sine term. The temperature difference, which is proportional to the heat-flow rate indicated above, is used as the response function for the heat capacity computation.

The total heat capacity of a sample with a pan can be determined by **Equation (19)**:

$$C_s = mC_p + C_p' = \frac{A_\varphi}{A_{T_b}\omega} \tag{19}$$

where C_p' is the heat capacity of the pan, A_Φ is the amplitude of the heat flow rate response of sample, A_{Tb} is the amplitude of the sinusoidal sample temperature modulation.

Since the sample and reference calorimeters show a phase shift in their response, the reversing heat capacity at steady-state from TM can be determined by Equation (20) [35]:

$$(C_s - C_r) = \frac{A_{\Delta T}}{A_{T_s}}\sqrt{\left(\frac{K}{\omega}\right)^2 + {C_r}^2} \tag{20}$$

where C_r is the heat capacity of the reference, which is equal to $C_p^{'}$ when it consists of an identical empty pan as the sample calorimeter, $A_{\Delta T}$ and A_{Ts} are the maximum amplitudes of the modulation in the temperature difference and sample temperature, respectively.

Then, Equation (20) can be expressed as:

$$mC_p = \frac{A_\Phi}{A_{T_s}\omega}\sqrt{1+\left(\frac{C_r\omega}{K}\right)^2} \quad (21)$$

The heat capacity is the quantity determined by Equation (17) from a TL scan, extracted from the TM scans, and an underlying heating rate $< \beta > 0$.

In this research, a periodical step-scan signal, which is a special sawtooth mode, is superimposed on the linear temperature changes yielding a heating profile, as shown in Fig. 5. The average temperature of a sample changes continuously with time in a non-linear fashion. After changing the sample mode by 1 °C at a particular modulation period and heating rate, the heat flow rate can equilibrate again. The underlying heating rate (5 °C/min) through the TM scans was minimal to separate the TL data from the dynamic controlled one. In nitrogen environment, the samples were first kept at −60 °C for 5 min and then heated up to 300 °C with 5 °C/min rate to investigate the glass transition changes over heating and the heat flow released due to the exothermic curing reactions in thermosetting binders. Then, after equilibrating the samples for 5 min at 300 °C, a cooling cycle was performed (to −60 °C with 5 °C/min cooling rate) and heated up again under the same modulation and scanning rate. Based on a Discrete Fourier Transformation, the measured amplitudes of temperature and heat flow modulation are compared to a reference signal of the same periodic characteristics calculating thus the heat capacity. All the C_p calculations were performed using the StepScan function in Pyris software (PerkinElmer).

3.2.2. Determination of heat of mixing

Over the 1st heating cycle from −60 °C to 300 °C, the samples are curing. After the termination of this cycle, the values of the total heat of reaction associated with complete chemical conversion are obtained by integrating the area between the maximum temperature of the exothermic peak of samples and the baseline, as illustrated in a schematic graph in Fig. 6. In the same figure, the DSC thermograph of a curing sample is also shown to emphasize the exotherm heat of mixing.

3.2.3. Determination of glass transition temperatures

Stepwise increase of heat capacity, specific volume, and stiffness modulus happen over the glass transition region from an amorphous to a glassy state. As mentioned, the glass transition most often is reported with the single value of T_g. Here, the sigmoidal change of C_p (or ΔC_p) in the glass-to-amorphous transition is monitored with the method introduced above to detect the T_g values of studied materials. The T_g values were determined as the temperature at the half-height between the onset and endpoint of the glass transition region, as depicted in Fig. 7**a**. The DSC thermograph of the epoxy system over the 1st heating cycle (curing system) and the 2nd heating cycle (cured system) from −60 °C to 300 °C is presented in Fig. 7**b**.

The Fox equation (14) was implemented to predict the $T_{g,mix}^{eq}$ and the magnitude of deviation from the ideal mixing theory. This equation is expressed as:

$$\frac{1}{T_{g,mix}^{eq}} = \frac{\varphi_A}{T_{g,A}} + \frac{\varphi_B}{T_{g,B}} \quad (22)$$

4. Results

Fig. 8 demonstrates the heat of mixing as a function of the binders composition. The heat of mixing was negative ($\Delta H_{mix} < 0$) throughout the composition range, as expected, since the curing reaction of the epoxy system is exothermic. Larger values of negative heat of mixing were observed in Binder 1 (i.e., 50 % EMA Binder 1: −65.59 J/g) comparing Binder 2 (i.e., 50 % EMA Binder 2: −35.60 J/g) (see Fig. 8**a**), indicating that higher energy levels were released over curing for the 20 % and 50 % diluted versions of Binder 1. A similar shape in ΔH_{mix} of binders versus the proportion of epoxy system is depicted in Fig. 8**b**, where the same versions of Binder 3 have shown slightly higher negative values of released heat due to curing (i.e., 50 % EMA Binder 3: −21.78 J/g) than of Binder 4 (i.e., 50 % EMA Binder 4: −17.62 J/g).

The ΔH_{mix} values decreased steeply with reducing the concentration of the epoxy system in asphalt, which is unfavorable for their miscibility. The concentration decrease in the epoxy system causes a dilution of the curing compounds in the asphalt binders and, thus, a reduction in the total exothermic heat evolved in curing. A proportion of curing epoxy compounds was wrapped in the asphalt phase; hence their mobility is reduced, and subsequently, it becomes difficult for the reactive compounds to participate in the crosslinking chemical reaction. It should be noted that the base Binder 3 and Binder 4, which are normally used for flexible pavement surfacing materials in the US, demonstrated comparable ΔH_{mix} values despite the fact they were of different sources.

The composition dependence of $T_{g,mix}$ of binders obtained from the C_p curves during glass transition, is shown in Fig. 9**a, 9b, 9c, and 9d**. The $T_{g,mix}$ values increase with the increase of the epoxy system in Binder 1, Binder 2, Binder 3, and Binder 4 after curing, as demonstrated in Fig. 9**a, 9b, 9c, and 9d**, respectively. On the one hand, before curing, the T_g values of the epoxy system and Binder 1 were –22.08 and −21.88 °C, respectively, yielding −15.47 and −20.86 °C for the 20 % and 50 % modification levels, respectively. This anomaly in the T_g – composition dependence of curing EMAs (i.e., 20 % and 50 % modification) is linked with the (thermal and mechanical) unstable state of these binders when the crosslink density of the modifier is low. Binary mixtures with components of nearly equal T_g values, as the curing EMAs, can show such attributes which might be associated with the development of steric hindrances between weakly interacting components. The

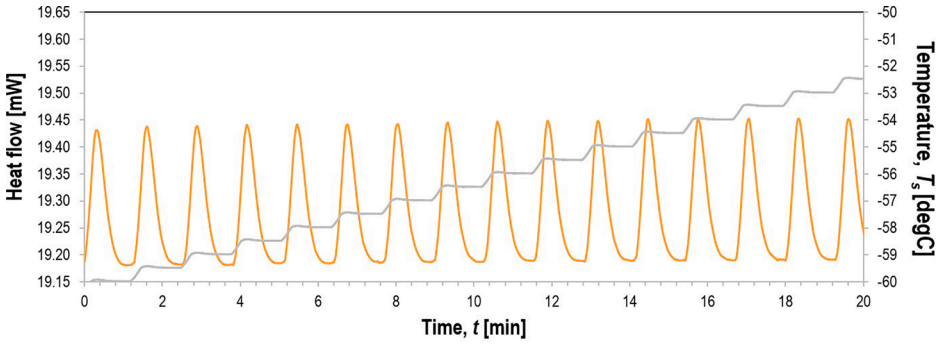

Fig. 5. TM-DSC profile of neat asphalt binder and the respective heat flow generated versus time (grey line represents the sample temperature (T_s) and the orange one the heat flow).

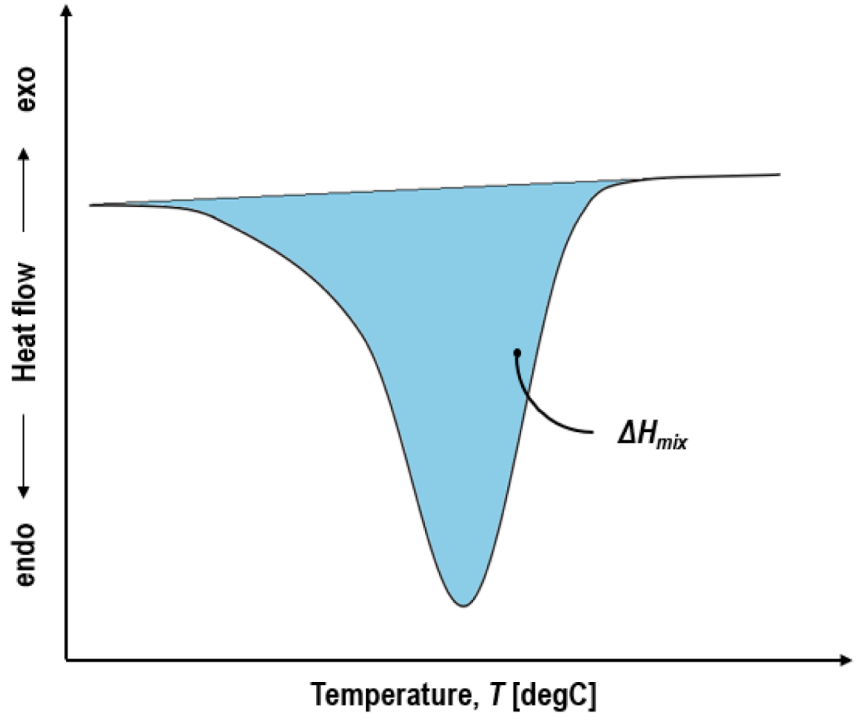

(a)

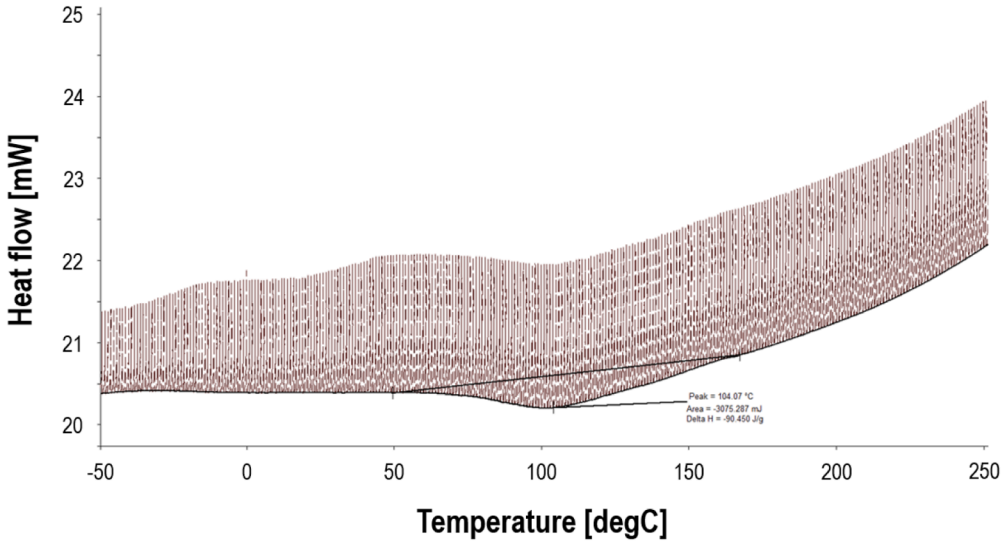

(b)

Fig. 6. Heat flow versus temperature: (a) schematic illustration, and (b) calorimetric results.

low magnitude of T_g values also implies the high potential segmental mobility between components of the binders. On the other hand, the T_g values of the cured epoxy, 50 %, and 20 % EMA Binder 1 were 16.33, −3.82, and −1.35 °C, respectively (Fig. 9**a**). The T_g changes that occurred with replacing the epoxy in Binder 2 were identical to those observed in Binder 1. Nevertheless, the T_g values of 20 % epoxy-modified Binder 2 were slightly lower than the 20 % epoxy-modified Binder 1 (Fig. 9**b**). Similar composition dependence of glass transition is observed in cured Binder 3 and Binder 4 but with significantly higher T_g values for the 50 % diluted versions (i.e., cured 50 % EMA Binder 3: 6.64 °C; and Binder 4: 7.60 °C) than of the cured 50 % epoxy-modified Binder 1 (i.e., cured 50 % EMA Binder 1: 0.29 °C).

The corresponding ΔC_p values were plotted in Fig. 9**a, 9b, 9c, and 9d**. The ΔC_p values determined with the above method were shifted to lower values with the epoxy system crosslinking through the same composition dependence profile. The ΔC_p values for Binder 1, Binder 2, Binder 3, Binder 4, the curing and cured epoxy binder were 0.38, 0.31, 0.27, 0,16, 0.24, and 0.15 J/(g·°C), respectively. In the same figure, the black and light dotted lines show the ideal mixing condition predicted by **Equation (22)**. Considering the $T_{g,mix}$ values at the ideal mixing condition, the deviation is positive and large for all binders. This attribute of positive $T_{g,mix}$ deviation becomes immediately visible after the

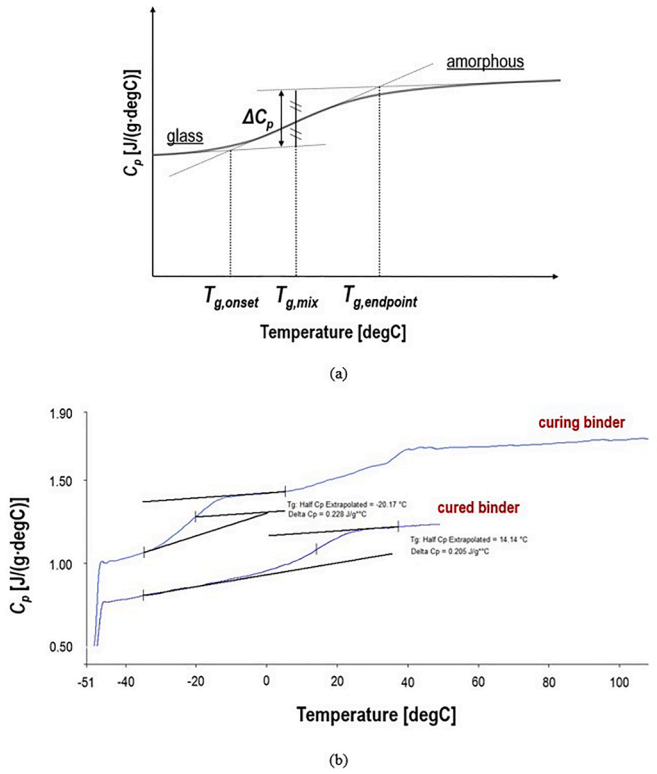

Fig. 7. Heat capacity changes over glass transition: (a) schematic illustration and (b) calorimetric results.

completion of crosslinking of the epoxy system in a nitrogen environment. The positive deviations of $T_{g,mix}$ obtained from the ideal mixing rule, or the positive values of $\Delta T_{g,mix}$, dictate the strong internal repulsive forces between the individual components.

The positive values of $\Delta T_{g,mix}$ leads to negative ΔS^c_{mix} values according to **Equation (15)**, a phenomenon which is illustrated in Fig. 10. Although the epoxy system causes positive deviations of $T_{g,mix}$, a softer base asphalt binder, such as Binder 2, is associated with a lower positive deviation of the relative $T_{g,mix}$ difference, and subsequently to a miscible system. After the crosslinking in the nitrogen environment, the contribution of the configurational entropy of mixing of the diluted versions of Binder 3 and Binder 4 was also calculated, showing higher values in Binder 4 than Binder 3, also manifesting higher repulsive forces between constituents. This attribute also dictates that the EMA binders produced using Binder 4 could be more thermodynamically unstable and, subsequently, immiscible than those developed using Binder 3.

A schematic representation of the epoxy effect on asphalt binders is depicted in Fig. 11, showing the changes of ΔS^c_{mix} and $T_{g,mix}$. The ΔS^c_{mix} manifests the magnitude change of $T_{g,mix}$. The replacement of asphalt binder by the epoxy system decreases the amount of ΔS^c_{mix} and increase the T_g of binder from $T_{g,mix}$ to $T_{g,mix\text{-}epoxy}$. Such performance dictates incompatible constituents and the formation of immiscible binders. For binders with small ΔS^c_{mix}, the $\Delta T_g/T_g$ is also small, and the systems are more homogeneous, as when liquid or functionalized additives are incorporated in binders to promote miscibility. The theory introduced in this research and its implementation could be the framework for a more precise characterization for selecting binders for flexible pavements.

5. Conclusions

The glass transition as a function of composition reflects the miscibility, or lack of it, in asphalt binders. In this study, a quantitative assessment of the contribution of thermodynamics of mixing to the glass transition of four epoxy-modified asphalt binders was performed in a differential scanning calorimetry. The main findings are as follows:

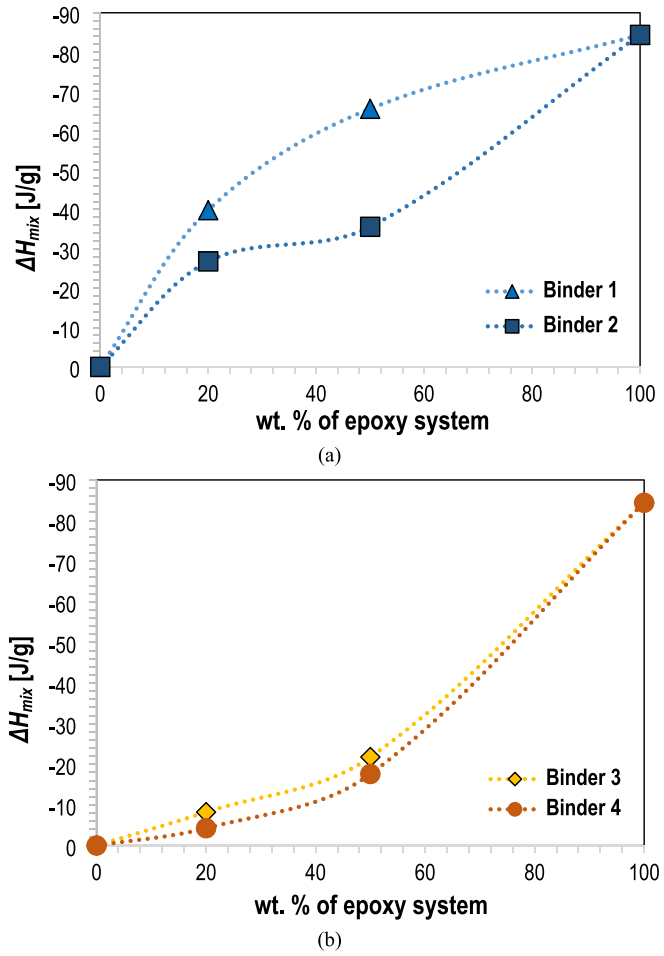

Fig. 8. Composition dependence of the ΔH_{mix} of binders: (a) Binder 1 & Binder 2, (b) Binder 3 & Binder 4.

- The ΔH_{mix} values increased steeply with increases in the amount of epoxy system in asphalt binders. In other words, a reduction in the quantity of epoxy causes a dilution of curing compounds in asphalt binders and, thus, a decrease in the total exothermic heat evolved in curing.
- The T_g values of asphalt binders partially replaced by the epoxy system were determined to quantify the miscibility via the entropic changes during glass transition. The $T_{g,mix}$ values increased with the increase of the epoxy system in asphalt binders after curing. Similar compositional dependence of glass transition is observed in cured binders but with variations in the extent of the T_g values as a result of the base asphalt binders employed.
- The positive deviations of $T_{g,mix}$ obtained from the ideal mixing rule, or $\Delta T_{g,mix}$, led to negative values of entropy of mixing (ΔS^c_{mix}) dictating the presence of strong internal repulsive forces between epoxy and asphalt. The softer binder is associated with a lower positive $\Delta T_{g,mix}$ and hence to a less immiscible product.

In the future, additional comprehensive studies are needed to elucidate the contribution of various other additives and agents to the phase behavior of petroleum- and non-petroleum-based binders toward an effort to develop sustainable flexible pavements.

CRediT authorship contribution statement

Panos Apostolidis: Conceptualization, Formal analysis,

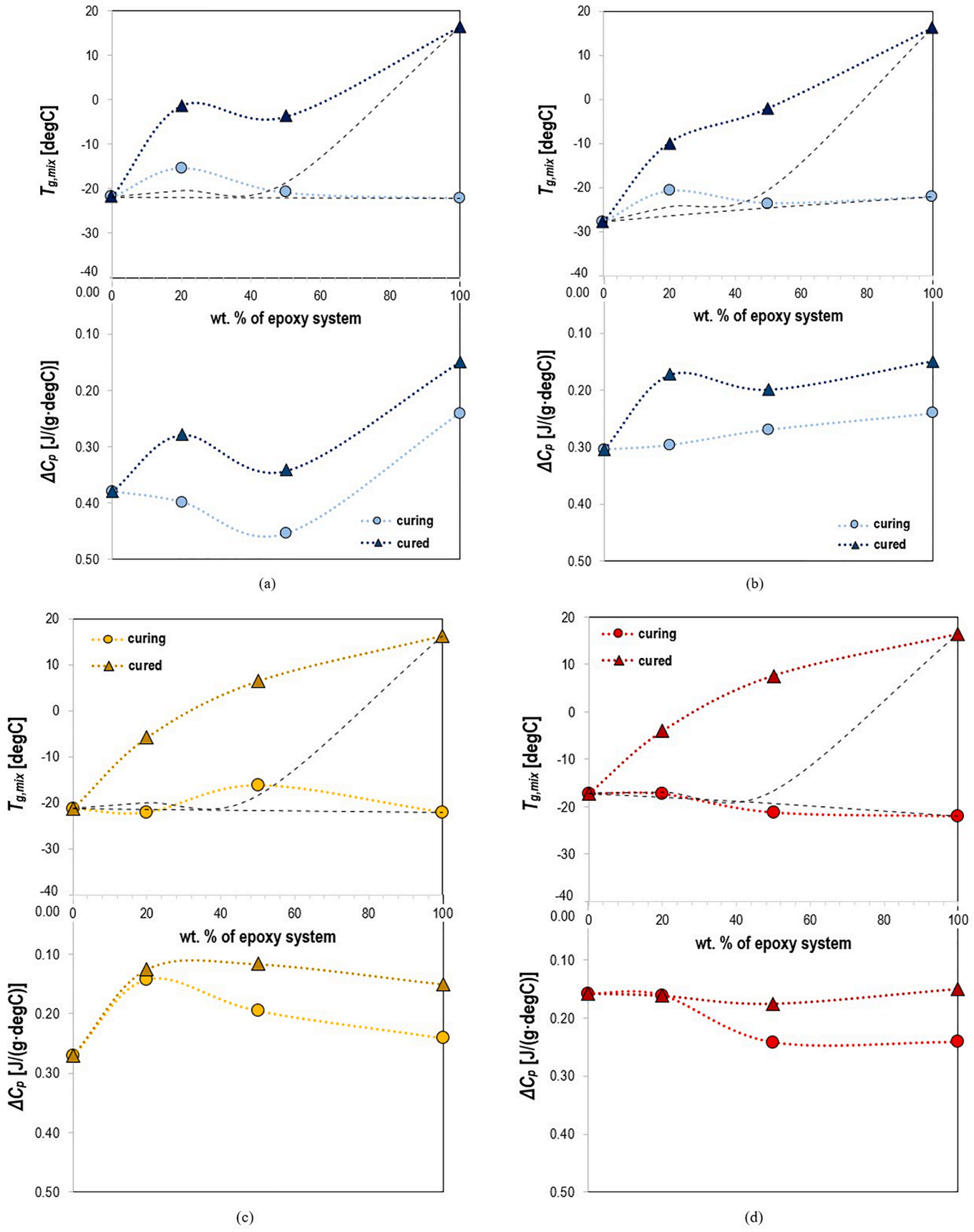

Fig. 9. Composition dependence of the $T_{g,mix}$ (top) and ΔC_p (bottom) of binders: (a) Binder 1, (b) Binder 2, (c) Binder 3 and (d) Binder 4 (black dashed lines corresponds to the ideal blends).

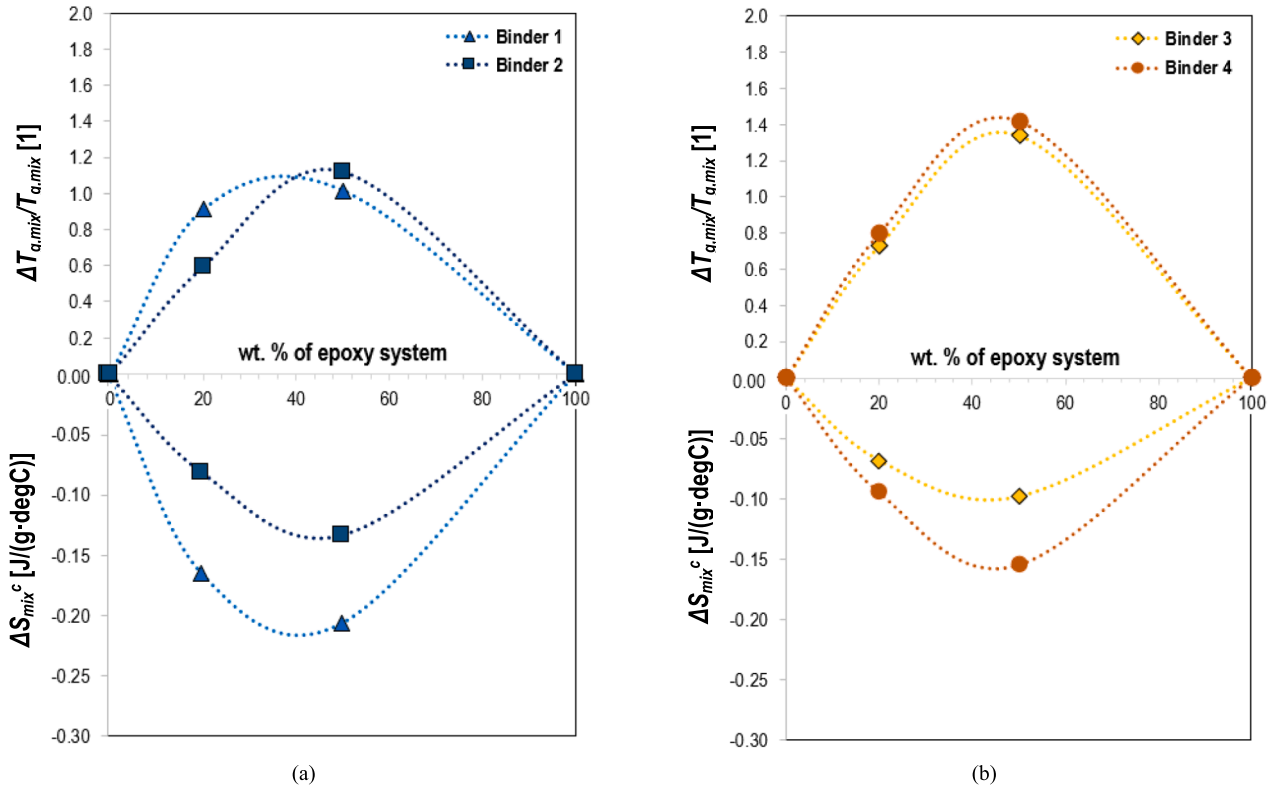

Fig. 10. Composition dependence of the $\Delta T_{g,mix}/T_{g,mix}$ (top) and the ΔS^{c}_{mix} (bottom) of binders: (a) Binder 1 & Binder 2, (b) Binder 3 & Binder 4.

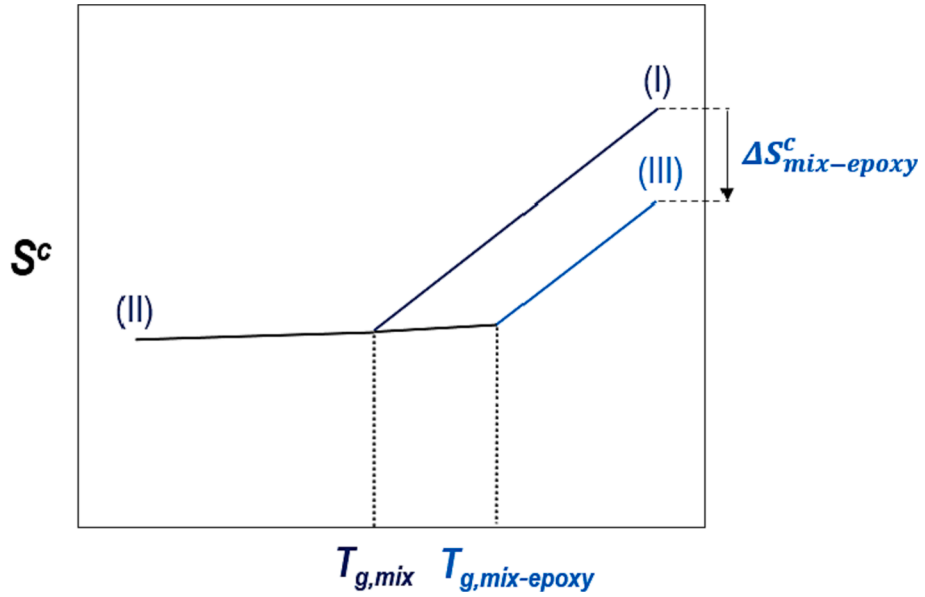

Fig. 11. The epoxy effect on asphalt binders (Lines (I) and (III) represent the neat binder and the modified binder at amorphous state, respectively. Line (II) represents the binder at glassy state).

Methodology, Writing – original draft. **Michael Elwardany:** Validation, Writing – original draft. **Adrian Andriescu:** Validation. **David J. Mensching:** Validation, Writing – original draft. **Jack Youtcheff:** Methodology.

Declaration of Competing Interest

The authors declare that they have no known competing financial interests or personal relationships that could have appeared to influence the study reported in this paper.

Data availability

Data will be made available on request.

References

[1] P.J. Flory, Principles of Polymer Chemistry, Cornell University Press, Ithaca, N.Y., 1953.
[2] M.M. Coleman, J.F. Graf, P.C. Painter, Specific Interactions and the Miscibility of Polymer Blends, CRC Press, Taylor & Francis Group, 1991.
[3] J.-F. Masson, P. Collins, G. Robertson, J.R. Woods, J. Margeson, Thermodynamics, Phase Diagrams, and Stability of Bitumen-Polymer Blends, Energy Fuel 17 (3) (2003) 714–724.
[4] P. Redelius, Bitumen Solubility Model using Hansen Solubility Parameter, Energy Fuel 18 (4) (2004) 1087–1092.
[5] P. Painter, B. Veytsman, J. Youtcheff, Phase Behavior of Bituminous Materials, Energy Fuel 29 (11) (2015) 7048–7057.
[6] J.-F. Masson, G. Polomark, P. Collins, Glass Transitions and Amorphous Phases in SBS-Bitumen Blends, Thermochim Acta 436 (1-2) (2005) 96–100.
[7] P. Apostolidis, M. Elwardany, L. Porot, S. Vansteenkiste, E. Chailleux, Glass Transitions in Bituminous Binders, Mater. Struct. 54 (2021) 132.
[8] P. Apostolidis, Chemo-Mechanics of Epoxy-Asphalt, Delft University of Technology, 2022. PhD Dissertation.
[9] H. Bahia, Low-Temperature Isothermal Physical Hardening of Asphalt Cements, The Pennsylvania State University, 1992. PhD Dissertation.
[10] D.A. Anderson, D.W. Christiansen, H.U. Bahia, R. Dongre, M.G. Sharma, C.E. Antle, J. Button, Binder Characterization and Evaluation, *Physical Characterization.* SHRP-A-369 Volume 3 (1994).
[11] D.A. Anderson, M.O. Marasteanu, Physical Hardening of Asphalt Binders Relative to their Glass Transition Temperatures, In *Transportation Research Record* 1661 (1) (1999) 27–34.
[12] M.D. Elwardany, J.-P. Planche, J.J. Adams, Determination of Binder Glass Transition and Crossover Temperatures using 4-mm Plates on a Dynamic Shear Rheometer, In *Transportation Research Record* 2673 (10) (2019) 247–260.
[13] M. Gordon, J.S. Taylor, Ideal Copolymers and the Second-Order Transitions of Synthetic Rubbers. I. Non-Crystalline Copolymers, J. Appl. Chem. 2 (9) (1952) 493–500.
[14] T.G. Fox, Influence of Diluent and Copolymer Composition on the Glass Temperature of a Polymer System, Bull. Am. Phys. Soc. 1 (1956) 123.
[15] A.V. Lesikar, Effect of Association Complexes on Glass Transition in Organic Halide Mixtures, J. Phys. Chem. 80 (1976) 1005–1011.
[16] P.R. Couchman, F.E. Karasz, A Classical Thermodynamic Discussion of the Effect of the Composition on Glass-Transition Temperatures, Macromolecules 11 (1978) 117–119.
[17] P.R. Couchman, Compositional Variation of Glass-Transition Temperatures. 2. Application of the Thermodynamic Theory to Compatible Polymer Blends, Macromolecules 11 (6) (1978) 1156–1161.
[18] P.R. Couchman, The Composition-Dependent Glass Transition: Relations between Temperature, Pressure, and Composition, Polym. Eng. Sci. 24 (2) (1984) 134–143.
[19] T. Kwei, The Effect of Hydrogen Bonding on the Glass Transition Temperature of Polymer Mixtures, J. Polym. Sci., Polym. Lett. Ed. 22 (1984) 307–313.
[20] L.A. Utracki, Glass Transition Temperature in Polymer Blends, Adv. Polym. Tech. 5 (5) (1985) 33–39.
[21] H.A. Schneider, E.A. Di Marzio, The Glass Temperature of Polymer Blends: Comparison of both the Free Volume and the Entropy Predictions with Data, Polymer 33 (16) (1992) 3453–3461.
[22] H.A. Schneider, Conformational Entropy Contributions to the Glass Temperature of Blends of Miscible Polymers, J. Res. Nat. Inst. Stand. Technol. 102 (1997) 229–248.
[23] E.A. Di Marzio, The Glass Temperature of Polymer Blends, Polymer 31 (12) (1990) 2294–2298.
[24] P.C. Painter, J.F. Graf, M.M. Coleman, Effect of Hydrogen Bonding on the Enthalpy of Mixing and the Composition Dependence of the Glass Transition Temperature in Polymer Blends, Macromolecules 24 (20) (1991) 5630–5638.
[25] S.S.N. Murthy, M. Tyagi, Dielectric Study of the Miscibility of Binary Liquids, One being an Alcohol, J. Solution Chem. 31 (2002) 33–58.
[26] R. Pinal, Entropy of Mixing and the Glass Transition of Amorphous Mixtures, Entropy 10 (2008) 207–223.
[27] P.K. Gupta, J.C. Mauro, Composition Dependence of Glass Transition Temperature and Fragility. I. A Topological Model Incorporating Temperature Dependent Constraints, J. Chem. Phys. 130 (9) (2009) 094503.
[28] I.M. Kalogeras, W. Brostow, Glass Transition Temperatures in Binary Polymer Blends, J Polym Sci B 47 (1) (2009) 80–95.
[29] L.-M. Wang, Y. Tian, R. Liu, K.L. Ngai, Anomalous Component Dynamics of a Binary Mixture of Associating Glass-Forming Liquids, J. Phys. Chem. B 115 (4) (2011) 719–724.
[30] I.M. Kalogeras, Description and Molecular Interpretations of Anomalous Compositional Dependences of the Glass Transition Temperatures in Binary Organic Mixtures, Thermochim Acta 509 (1-2) (2010) 135–146.
[31] W. Kauzmann, The Nature of the Glassy State and the Behavior of Liquids at Low Temperatures, Chem. Rev. 43 (2) (1948) 219–256.
[32] Goldstein, M. Viscous Liquids and Glass Transition. 7. Molecular Mechanisms for a Thermodynamic 2nd Order Transition. *The Journal of Chemical Physics 67*, 1977, pp. 2246-53.
[33] B. Wunderlich, M. Pyda, Application of the Advanced THermal Analysis System (ATHAS) to Differential Scanning Calorimetry (DSC) and Temperature Modulated DSC of Polymers, J. Reinforced Plastics and Composites 18 (6) (1999) 487–498.
[34] P.S. Gill, S.R. Sauerbrunn, M. Reading, Modulated Differential Scanning Calorimetry, J. Thermal Anal. 40 (3) (1993) 931–939.
[35] B. Wunderlich, Y. Jin, A. Boller, Mathematical Description of Differential Scanning Calorimetry Based on Periodic Temperature Modulation, Thermochim. Acta 238 (1994) 277–293.